Singlet fission in linear chains of molecules

Francesco Ambrosio* and Alessandro Troisi*

Department of Chemistry and Centre for Scientific Computing, University of Warwick, UK

*E-mail: F.Ambrosio@warwick.ac.uk A.Troisi@warwick.ac.uk

Abstract

We develop a model configuration interaction Hamiltonian to study the electronic structure of a chain of molecules undergoing singlet fission. We first consider models for dimer and trimers and then we use a matrix partitioning technique to build models of arbitrary size able to describe the relevant electronic structure for singlet fission in linear aggregates. We find that the multi-excitonic state (ME) is stabilized at short inter-monomer distance and the extent of this stabilization depends upon the size of orbital coupling between neighboring monomers. We also find that the coupling between ME states located on different molecules is extremely small leading to bandwidths in the order of ~10meV. This observation suggests that multi-exciton states are extremely localized by electron-phonon coupling and that singlet fission involves the transition between a relatively delocalized Frenkel exciton and a strongly localized multi-exciton state. We adopt the methodology commonly used to study non-radiative transitions to describe the singlet fission dynamics in these aggregates and we discuss the limit of validity of the approach. The results indicate that the phenomenology of singlet fission in molecular crystals is different in many important ways from what is observed in isolated dimers.

1. Introduction

Singlet fission (SF) is a special case of spin allowed transition, where a single-exciton singlet state (usually S_1) splits in two coupled single-exciton triplet (T_1) excitations.[1, 2] Decades after its first observation in anthracene crystals, SF has been recently experimented in a wide variety of crystalline organic materials,[3-10] polymers,[11] quantum dots,[12] and in solution.[13] One of the reasons behind a renewed interest on this physical phenomenon is given by the opportunity to exploit it, in order to overcome the Shockley-Queisser theoretical limit of conversion efficiency for single junction solar cells,[14] a possibility that has been verified in few instances[4, 15] but it is still under debate.[16]

SF is a thermodynamically favorable process when the following condition is satisfied[1]:

$$E(\mathrm{S}_1) > 2E(\mathrm{T}_1) \tag{1}$$

where, for isolated molecular pairs, $E(\mathrm{S}_1)$ and $E(\mathrm{T}_1)$ represent the energy of the first singlet and triplets states, respectively, while for crystalline materials represent the bottom of the singlet and triplet bands, respectively. Eq. (1) is true for organic crystalline materials like pentacene and hexacene derivatives, the former being the most studied material for SF purposes.[3, 9, 17-25] For hexacene, instead, a possible fission of the singlet in three triplets has been recently proposed, due to the extremely low energy of T_1.[26] However, hexacene is very unstable[27] and, for this reason, is usually functionalized.[28, 29] For these crystalline organic materials, the production of two separate triplets is an ultrafast process ranging from hundreds of fs (pentacene) to ps (hexacene).[24, 25] However, a recent joint experimental and theoretical work by Busby and coworkers estimated a rate for SF in hexacene of 540 fs, and proposed that SF in this material occurs with the formation of two separated triplets and the emission of high energy phonons, instead of the formation of three separated triplets.[30] In other materials, i.e. tetracene, the previous condition is not met and SF is a thermally activated and slower process. Burdett and Bardeen studied the temperature-dependence for the decay of singlet exciton in tetracene crystals, in particular at low temperatures (200 K), where it is affected by a possible change of polymorphism.[5, 6] However, Friend's group suggests that the generation of triplet pairs, in absence of the driving force given by exothermicity, is due to an equilibrium-like process between S_1 and $2T_1$ populations, thus explaining both lower rates and high quantum yield.[3]

It is known that the mechanism of SF features an intermediate state which is typically described by a doubly excited configuration where two triplets with opposite spins are accommodated on two

different excitation sites. This state is referred in literature as ^{1}(TT) or, more commonly, as multi-excitonic (ME) state.[1, 2] Its overall spin multiplicity is a singlet, and hence the process is spin allowed. SF can be described as a two steps process:

$$S_1 \rightarrow ME \rightarrow T_1 + T_1 \quad (2)$$

Experimental proof of existence of this dark state has been recently obtained via time-resolved two-photon photoemission spectroscopy for the pentacene/C_{60} system.[22]

A main controversy in SF mechanism arises from the coupling between ME and S_1 states: some studies suggest that the main interaction driving the ME←S_1 transition is the direct coupling between these two states;[5, 17, 18, 31] another school of thought indicates that direct coupling is not sufficient to explain the rates of SF and suggests that indirect coupling via charge transfer (CT) states causes the ultra-fast dynamics of ME generation.[32-35]

Zimmermann *et al.* employed post-HF methods to study a pentacene dimer model. The ME state was characterized as the intermediate state leading to SF. It has been found that ME←S_1 transition is fast and the subsequent separation in $2T_1$ is favoured by the formation of an excimer-like complex.[17] In a successive paper, Zimmermann *et al.* also studied pentacene and tetracene through QM/MM calculations, adopting the RAS-2SF method;[36] his results suggest that ME←S_1 transition is driven by the direct coupling between them and no CT state is involved in the process.[18] Zhu's group argues that the ultrafast dynamics arising from available experiments cannot be justified by direct coupling between S_1 and ME. Multi-state DFT and density matrix modeling were employed to show that indirect coupling through CT states is two orders of magnitude higher than direct coupling. This should justify the ultrafast dynamics, in conjunction with high density of ME states and dephasing produced by environmental effects.[32] Casanova studied tetracene and two of its derivatives with *ab initio* quantum chemical calculations, excluding in all the cases the role of CT states as possible intermediates of the SF mechanism, but confirming their role for second order coupling.[37] Recently, Van Voorhis group calculated the energy levels and the electronic coupling between S_1 and a TT state for dimers belonging to the crystallographic structures of different pentacene and tetracene derivatives, using constrained DFT (CDFT) and CDFT based configuration interaction (CDFT-CI).[38] Rates of SF, following the scheme proposed by Bixon and Jortner,[39-41] were in agreement with experimental results.[42] Regarding the mechanism, it is proposed that, for weakly interacting systems, SF is non-adiabatic while it is adiabatic for strongly coupled systems.[42] Finally, in a very recent contribution from Shiozaki's group, an accurate approach for building model Hamiltonians for dimer systems, from *ab initio* calculations, was proposed. Dimer electronic

states were expressed as linear combination of monomer wave functions, the latter being computed from RAS calculations.[43]

Recently, theoretical studies have also been carried out, in order to investigate the interface between the SF material and the donor material in an organic solar cell (OSC). Prezhdo's group studied the C_{60}-pentacene interface. A kinetic model for SF was derived from non-adiabatic molecular dynamics, where a simulation cell composed by two pentacene molecules and a C_{60} molecule was adopted. They found that SF in a typical interface of an OSC must compete with the usual mechanism of exciton dissociation at the donor-acceptor interface.[44] This agrees with previous studies, motivating the competition between SF and exciton dissociation at the interface, for C_{60}-pentacene and C_{60}-tetracene systems, and showing that SF is favored for pentacene but not for tetracene.[45] However, a critical point of non-adiabatic dynamics is given by the fact that it forces the system into one of the adiabatic potential energy surfaces via a sequence of fast hops, while, for very fast processes it is more likely for the system to be in a linear combination of electronic states.

Over the past few years, Reichman's group developed a phenomenological model based on a minimal CI Hamiltonian, describing the pentacene dimer. The quantum dynamics of SF was studied, considering only the electronic degrees of freedom explicitly, while all nuclear modes are part of a bath system, using Redfield theory.[46] The results for this kind of approach suggest that SF occurs via a "super-exchange" mediated mechanism, through CT states, even if these states possess very high energies.[32-34] Very recently, Reichman's group extended the application of this theoretical framework to the study of crystalline pentacene.[47] This was achieved with a combination of *ab initio* calculations and semi-empirical modeling. The results were compared to the one obtained in their previous works on dimers;[33, 34] while they found the kinetics of SF being consistent with the one observed for the dimer case, a sensible qualitative difference between the two cases was noted. According to their calculations, in crystalline pentacene, CT states are largely mixed (~50%) with Frenkel exciton states and, hence, SF in this case should occur via a single electron transfer process.[47] Feng *et al.* criticize the diabatization approach of Reichman's group in ref.[33, 34] and they propose the use of adiabatic wave-function and the calculation of non-adiabatic couplings. In this way, they argue that there is no need to introduce concepts like "super-exchange" or "two electron coupling", as the CT configurations are already included in S_1 and ME wave-functions.[48] In a similar approach, Beljonne *et al.* developed a phenomenological Hamiltonian in conjunction with quantum chemical calculations, in order to study the photophysics of pentacene. They state that the lowest singlet exciton has a huge contribution (up to 50%) from CT configurations and this is the main responsible for Davydov splitting in pentacene. Also ME has a similar contribution from CT

excitations; therefore, S1 and ME can be almost simultaneously populated when close in energy. Either wise, fast SF could still occur with a CT mediated mechanism.[23, 49] Nevertheless, recent calculations, performed on dimers of perylenediimide, pentacene and isobenzofuran with density matrix propagation, via Redfield theory, agree with the picture proposed by Reichman's group, confirming that a "super-exchange" mechanism mediated by CT states is responsible for SF rates.[35]

In this work, we would like to contribute to the understanding of single fission by exploring two directions. First, we consider the electronic structure of linear aggregates of molecules undergoing singlet fission to understand the main qualitative differences with respect to the dimer model. In sections 2.1-2.3 we start by considering a model Hamiltonian of dimer and trimer and we propose a scheme to construct model Hamiltonian of linear aggregates of arbitrary size (section 2.4) leading to non-trivial observations on the nature of multi-excitonic states (section 2.5). We then describe the process of singlet fission using the classical theoretical framework of non-radiative transition (section 3.1-3.2), and discuss the range of validity range of the model (section 3.3).

2. A model configuration interaction Hamiltonian for the study of the multi-excitonic states in singlet fission

2.1. CISD model for 1D aggregate

The starting point of our study of SF is a simple system of N sites (monomers). Each site j possesses two orbitals a^j and r^j that are respectively occupied and empty in the ground state, i.e. they represent the HOMO and LUMO of a molecule on site j. The two monomers are separated by a distance d. We choose to describe the electronic structure of this model system using CI theory, where the expansion of the CI wave function is truncated to doubles configurations (CISD). For a generic cluster of N monomers the wave function is given by:

$$\Phi = c_0|0\rangle + \sum_{ij}^{N} c_j^i \,|{}_i^j\rangle + \sum_{\substack{i<k \\ j<l}}^{N} c_{ik}^{jl} \,|{}_{ik}^{jl}\rangle \tag{3}$$

We introduced a simplified notation for the excited configurations: for single excitations, the notation $|{}_i^j\rangle$ indicates a single excited configuration from the HOMO orbital of the i-th monomer to the LUMO orbital of the j-th monomer while $|{}_{ik}^{jl}\rangle$ indicates a double excited configurations from

the HOMO orbital of monomers i and k to the LUMO orbitals of monomers j and l. In this work we make use of singlet spin-adapted configurations (rather than Slater determinants). Two non-equivalent singlet configurations exist for the double excitations $|\begin{matrix} jl \\ ik \end{matrix}\rangle$ and they will be discussed below as they are relevant for the ME state of interest.

It is important to remember that considering a two-orbital system is equivalent to neglecting a sensible amount of dynamic correlation energy. The effect of the neglected electronic states may result into a screening of some of the Hamiltonian matrix element as noted in ref.[33] and the screening itself may be dependent on the size of the cluster.

2.2. Parameterization of the model for dimer and trimer

In **Table 1** we list the parameters used for computing the matrix elements for the CI matrix, H_{CI}. In particular, we choose two sets of parameters: a tetracene-like (T) set of parameters and pentacene-like (P) one, meant to reproduce the energy of the S_1 state in the tetracene and pentacene isolated molecules and the separation between singlet and multi-exciton states observed in the tetracene and pentacene crystals.

(i) the orbital energies ε_{r} and ε_{a} are taken from experimental values of ionization potential and electron affinities whose have been reported from available literature;[50, 51]

(ii) intra-monomer coulomb integrals ($J_{\mathrm{r^i a^i}}$, $J_{\mathrm{r^i r^i}}$, $J_{\mathrm{a^i a^i}}$) represent Coulombic repulsion between two electrons which is expressed by the following bi-electronic integral (i.e. for $J_{\mathrm{r^i a^i}}$) :

$$J_{\mathrm{r^i a^i}} = \left(\mathrm{r^i r^i}\middle|\mathrm{a^i a^i}\right) = \iint \psi_{r^i}^2(x_1)\frac{1}{x_{12}}\psi_{a^i}^2(x_2)dx_1dx_2 \tag{4}$$

where x_{12} is the distance between the two electrons. We assume that all the integrals of this type ($J_{\mathrm{r^i a^i}}$, $J_{\mathrm{r^i r^i}}$, $J_{\mathrm{a^i a^i}}$) are equal to a common constant J. The latter is estimated from the expression of the triplet energy in a model with one site possessing two orbitals:

$$E(T_1) = \varepsilon_{\mathrm{r}} - \varepsilon_{\mathrm{a}} - J \tag{5}$$

Where ε_{r} and ε_{a} have been previously defined and $E(T_1)$ is taken from available literature as the energy of the low-lying triplet state in isolated pentacene and tetracene molecules.[1]

(iii) The exchange integral $K_{\mathrm{r^i a^i}}$, defined as

$$K_{\mathrm{r^i a^i}} = \left(\mathrm{r^i a^i}\middle|\mathrm{a^i r^i}\right) = \iint \psi^*_{r^i}(x_1)\psi_{a^i}(x_2)\frac{1}{x_{12}}\psi^*_{a^i}(x_1)\psi_{r^i}(x_2)dx_1dx_2 \quad (6)$$

was taken from available literature[1] to reproduce the experimental energy difference between S_1 and T_1 in the isolated monomer[1] which is twice the exchange integral in a model with only two orbitals per site. For simplicity we can denote this exchange integral simply as Kas there is no possibility of confusion with other matrix elements included in the model.

(iv) The inter-monomer coulomb integrals ($J_{\mathrm{r^i a^j}}$, $J_{\mathrm{r^j a^i}}$, $J_{\mathrm{r^i r^j}}$, $J_{\mathrm{a^i a^j}}$) represent the electronic repulsion for two electrons on different sites:

$$J_{\mathrm{r^i a^j}} = \iint \psi^2_{r^i}(x_1)\frac{1}{x_{12}}\psi^2_{a^j}(x_2)dx_1dx_2 \quad (7)$$

These matrix elements depend on the distance d between two monomers. For very large distance, the dependence should be Coulombic, i.e. proportional to $1/d$. These matrix elements have been parametrized by the following expression:

$$\frac{1}{4\pi\varepsilon_0} \times \frac{e^2}{\sqrt{(d^2 + l^2)}} \quad (8)$$

Where l is an approximate measure of the size of the electronic cloud of tetracene and pentacene molecules, given by the length of the molecule (9.75 Å and 12.00 Å for tetracene and pentacene respectively). Eq. (8) reduces Coulomb repulsion when $d \gg l$.

(v) The matrix element $V_{ex} = (\mathrm{r^i a^i}|\mathrm{r^j a^j})$, known as the excitonic coupling, can be estimated for a dimer as the half of the splitting of the Frenkel excitonic states. In exciton theory, it is described by the interaction between two point dipoles separated by a distance d.[52] We set a reference excitonic coupling $V^0_{ex} = 0.15$ eV between two sites separated by $d_0 = 4$ Å, and hence for longer distances the following functional form is used:

$$V_{ex} = V^0_{ex}\left(\frac{d^3_0}{d^3}\right) \quad (9)$$

(vi) Fock matrix elements ($F_{\mathrm{r^i a^j}}$, $F_{\mathrm{r^j a^i}}$, $F_{\mathrm{r^i r^j}}$,$F_{\mathrm{a^i a^j}}$) decrease exponentially with increasing distance between site i and j. We use a single parameter $F' = 0.15$ eV for all matrix elements of this type[53] involving adjacent molecules. The matrix element is set to zero for non-adjacent molecules. If one is interested in a specific system it is important to remember that the sign as well as the magnitude

of the different Fock matrix elements influences the system observables.[34] To verify that our simplified choice of identical positive Fock matrix elements does not influence the essential physics discussed here some key quantities have been recomputed using different sign of the Fock matrix element or keeping the signs all positive while changing the magnitude of F'. The results of these tests are discussed in section 3.

(vii) In a trimer, the Hamiltonian matrix is also dependent on the integral $(a^i a^j|r^i r^j)$ which is responsible of the energy splitting between the two lowest triplets in a dimer system, originating from the triplet states on the monomers. These elements, non-vanishing only if $|i-j|=1$, have been set to 0.05 eV for tetracene and 0.015 eV for pentacene. These values correspond to the largest triplet-triplet splitting computed at TD-DFT/B3LYP/6-31G* level between various non-equivalent pairs of adjacent molecules in the corresponding molecular crystal.

Table 1: List of parameters needed to define the CI Hamiltonian and their values for P and T scenarios

Parameters	**Value (eV)**
$\varepsilon_r - \varepsilon_a$ (Ref.[50, 51])	5.9 eV (T), 5.2 eV (P)
J	4.75 eV (T), 4.33 eV (P)
K (Ref.[1])	0.55 eV (T), 0.72 eV (P)
V_{ex}^0 (Ref.[52])	0.15 eV (T,P)
F'	0.15 eV (T,P)
$(a^i a^{i+1}\|r^i r^{i+1})$	0.05 eV(T), 0.015 eV (P)

2.3. Comparison between dimer and linear trimer cases: bound and unbound ME states

The simplest possible cluster is a dimer model. In **Supporting Information** (**SI)**, we report the expression for the CISD Hamiltonian matrix elements in terms of the parameters defined in the previous section.

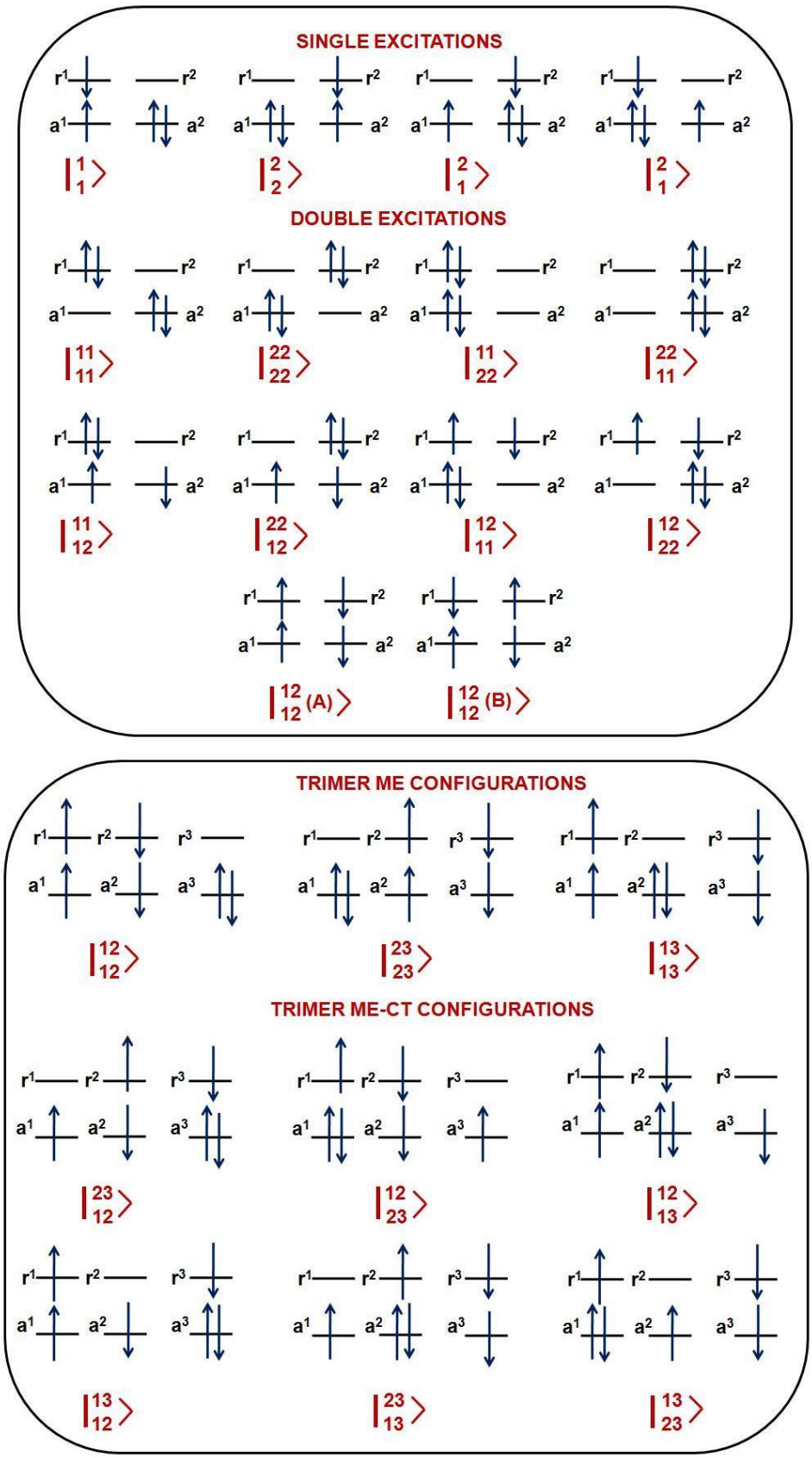

Figure 1: Schematic representation of singlet excited configurations for a dimer model (top panel) and of configurations of interest for the trimer case (bottom panel).

A schematic representation of the excited configurations is reported in **Figure 1** (top panel). Among the matrix elements, we underline that there are two different $|\begin{smallmatrix}12\\12\end{smallmatrix}\rangle$ excited state configurations, labeled as A and B. They differ because, as shown in **Figure 1**, $|\begin{smallmatrix}12\\12\end{smallmatrix}(\mathrm{A})\rangle$ is constituted by two triplets excited configurations (also called pseudo-triplets), one on each site, with opposite spin, thus granting an overall singlet nature to the configuration. On the other side, $|\begin{smallmatrix}12\\12\end{smallmatrix}(\mathrm{B})\rangle$ can be viewed as composed by a single singlet excitation on each site.

The energy levels for the states of interest, resulting from the diagonalization of the CISD Hamiltonian are reported in **Figure 2a** (the energy of the ground state configuration was set to zero).

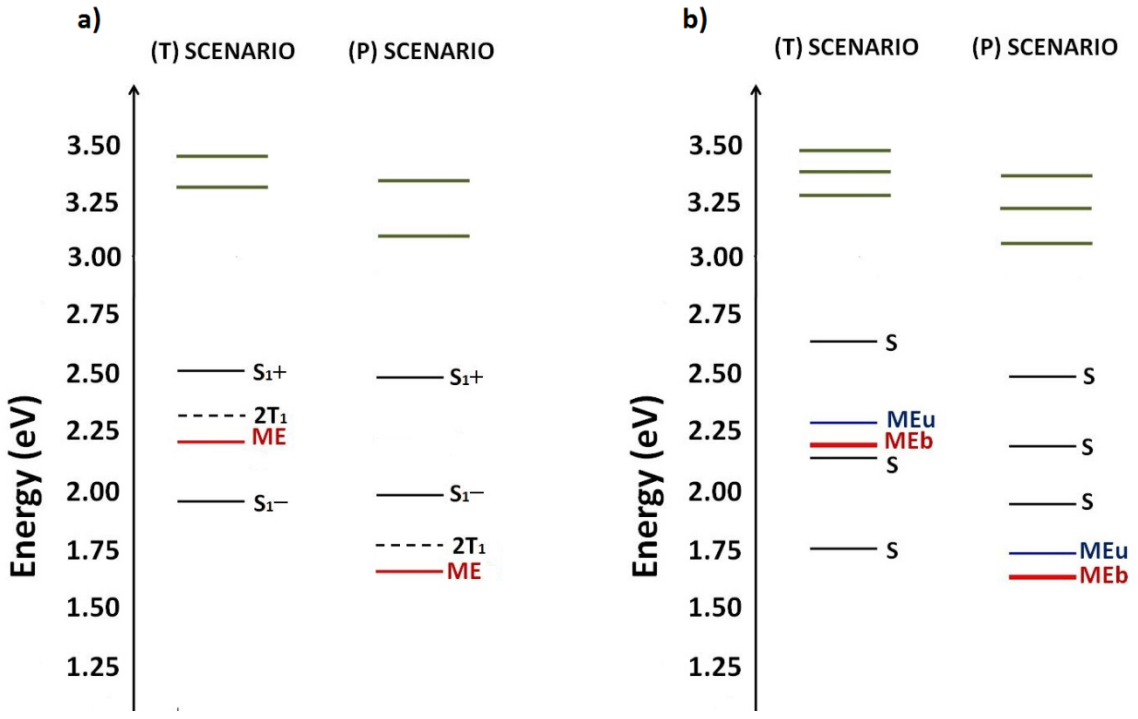

Figure 2: Eigenvalues of the states of interest of the dimer model for T and P scenarios for a) dimer model and b) trimer model. Dashed line correspond to the energy of two separated triplet states. In green we report the states nearest to the states of interest (see text for description).

We notice, for both set of parameters considered, two singlets states (labeled as $S_1{+}$ and $S_1{}^{-}$) constituted for more than 95% of the mixing of $|\begin{smallmatrix}1\\1\end{smallmatrix}\rangle$ and $|\begin{smallmatrix}2\\2\end{smallmatrix}\rangle$, which are coupled both directly

through V_{ex} and indirectly through CT determinants ($|\begin{smallmatrix}2\\1\end{smallmatrix}\rangle$, $|\begin{smallmatrix}1\\2\end{smallmatrix}\rangle$). The ME state is defined as the state with a predominant weight (>95%) of the $|\begin{smallmatrix}12\\12\end{smallmatrix}(A)\rangle$ configuration. The ME state is stabilized by the Fock elements which arise from the coupling of$|\begin{smallmatrix}12\\12\end{smallmatrix}(A)\rangle$ with singles and doubles charge transfer (CT) configurations ($|\begin{smallmatrix}2\\1\end{smallmatrix}\rangle$, $|\begin{smallmatrix}1\\2\end{smallmatrix}\rangle$, $|\begin{smallmatrix}21\\11\end{smallmatrix}\rangle$, $|\begin{smallmatrix}12\\22\end{smallmatrix}\rangle$, $|\begin{smallmatrix}11\\12\end{smallmatrix}\rangle$, $|\begin{smallmatrix}22\\12\end{smallmatrix}\rangle$). The ME state has energy ~0.08 eV lower than then the energy of two separated triplets, also reported in Figure 2. Other states are well separated in energy from our states of interest and do not mix much with them. The lowest ones are reported in green in **Figure 2a** and are given by linear combinations of $|\begin{smallmatrix}11\\11\end{smallmatrix}\rangle$ and $|\begin{smallmatrix}22\\22\end{smallmatrix}\rangle$ configurations. Lowest energy CT states (not appearing in figure) have higher energies, above 3.5 eV, somewhat higher than experimental estimations[48, 54], possibly due to an underestimation of J'.

As good as a starting point it might be, a dimer model is not capable of capturing the whole physics of a process taking place in a crystalline solid like pentacene or tetracene. If just a trimer model is considered instead of the dimer one, there will be new configurations appearing; in particular the two pseudo-triplets can be located on neighboring sites ($|\begin{smallmatrix}12\\12\end{smallmatrix}\rangle$,$|\begin{smallmatrix}23\\23\end{smallmatrix}\rangle$) as in the dimer case (we simplify the notation for these double excitations, since from now on we will only consider A-type configurations), but there is also a configuration where the two pseudo-triplets are separated: $|\begin{smallmatrix}13\\13\end{smallmatrix}\rangle$. Moreover, these different configurations couple among each other both directly, through a $(a^i a^j|r^i r^j)$ matrix element, and indirectly through new ME-CT states appearing in the system (see **Figure 1** – bottom panel).

The energies of the states of interest for P and T scenarios are shown in **Figure 2b**. The ME states of the trimer system are not at the same energy. In particular, we can divide the ME states in two sets: a first set at lower energy, which is composed by linear combinations of $|\begin{smallmatrix}12\\12\end{smallmatrix}\rangle$ and $|\begin{smallmatrix}23\\23\end{smallmatrix}\rangle$, two states which are almost degenerate; a second set contains in this case a single state dominated by the contribution of $|\begin{smallmatrix}13\\13\end{smallmatrix}\rangle$ configuration and it is approximately 0.1 eV higher in energy than MEb states, for both tetracene-like and pentacene-like scenarios. As the ME states formed by close excitations are at lower energy we can denote them as *bound* ME states or MEb. Conversely all the other ME states are denoted as *unbound* or MEu and the energy difference between MEu and MEb states can be thought of as the binding energy of the bound ME states.

2.4. From linear trimer to a chain of N molecules

The number of double configurations that should be included for clusters with a larger number of molecules increases rapidly (approximately as N^4) and becomes rapidly intractable. It would be desirable to build an effective model Hamiltonian for a chain of N monomers, containing only the N Frenkel-type excitons and the $N(N-1)/2$ ME states. To achieve this simplified description we start by using a matrix partitioning scheme for the trimer model, that generates an effective Hamiltonian for the trimer, containing only singlet and ME configurations.[55-57] All the other configurations contribute to the stabilization of the configurations of interest and can mediate the coupling between configurations of interest, both effects being captured by the partitioning method. The CISD Hamiltonian for the trimer model can be written in the following form[58]:

$$[H^{eff}_{3,\mathrm{CI}}]_{aa} = [H_{3,\mathrm{CI}}]_{aa} + [H_{3,\mathrm{CI}}]_{ab}(1E' - [H_{3,\mathrm{CI}}]_{bb})^{-1}[H_{3,\mathrm{CI}}]_{ba} \qquad (10)$$

where$[H_{3,CI}]_{aa}$ is the block of $H_{3,\mathrm{CI}}$ that corresponds to the configurations of interest (the three configurations leading to singlets S_1, S_2, S_3 and the three configurations leading to ME states: MEb1, MEb2 and MEu). $[H_{3,CI}]_{bb}$ is the block containing the matrix elements of all the other configurations. $[H_{3,CI}]_{ab}$ and $[H_{3,CI}]_{ba}$ contain all the coupling elements of the configurations of interest with all the other states. Finally, E' is a parameter which is chosen as the average of the eigenvalues of the states of interest from previous diagonalization of H_{CI}. Therefore $H^{eff}_{3,CI}$ is an effective Hamiltonian for the trimer model, including only the configurations of interest and the effective coupling due to the interaction among themselves and with all the other configurations.

The final step to obtain an effective Hamiltonian for a 1D aggregate of N monomers ($H^{eff}_{N,\mathrm{CI}}$) is made by establishing some rules to construct it from the matrix elements of $H^{eff}_{3,\mathrm{CI}}$.

(i) For the diagonal matrix elements involving the N singly excited configurations we set: $\left\langle {1 \atop 1}\middle| H^{eff}_{N,\mathrm{CI}} \middle| {1 \atop 1}\right\rangle \equiv \left\langle {1 \atop 1}\middle| H^{eff}_{3,\mathrm{CI}} \middle| {1 \atop 1}\right\rangle$, $\left\langle {N \atop N}\middle| H^{eff}_{N,\mathrm{CI}} \middle| {N \atop N}\right\rangle \equiv \left\langle {3 \atop 3}\middle| H^{eff}_{3,\mathrm{CI}} \middle| {3 \atop 3}\right\rangle$ and for the remaining $N-2$ configurations $\left\langle {i \atop i}\middle| H^{eff}_{N,\mathrm{CI}} \middle| {i \atop i}\right\rangle \equiv \left\langle {2 \atop 2}\middle| H^{eff}_{3,\mathrm{CI}} \middle| {2 \atop 2}\right\rangle$.

(ii) For the off-diagonal matrix elements involving the singly excited configurations we set: $\left\langle {i \atop i}\middle| H^{eff}_{N,\mathrm{CI}} \middle| {i+1 \atop i+1}\right\rangle \equiv \left\langle {1 \atop 1}\middle| H^{eff}_{3,\mathrm{CI}} \middle| {2 \atop 2}\right\rangle$, $\left\langle {i \atop i}\middle| H^{eff}_{N,\mathrm{CI}} \middle| {i+2 \atop i+2}\right\rangle \equiv \left\langle {1 \atop 1}\middle| H^{eff}_{3,\mathrm{CI}} \middle| {3 \atop 3}\right\rangle$ and, for $|i-j|>2$, $\left\langle {i \atop i}\middle| H^{eff}_{N,\mathrm{CI}} \middle| {j \atop j}\right\rangle \equiv V_{ex}(|j-i|d)$.

(iii) For the diagonal matrix elements involving doubly excited configuration we set:

$\left\langle {i, i+1 \atop i, i+1} \right| H^{eff}_{N,\mathrm{CI}} \left| {i, i+1 \atop i, i+1} \right\rangle \equiv \left\langle {12 \atop 12} \right| H^{eff}_{3,\mathrm{CI}} \left| {12 \atop 12} \right\rangle$ and for $|i-j|>1$ $\left\langle {ij \atop ij} \right| H^{eff}_{N,\mathrm{CI}} \left| {ij \atop ij} \right\rangle \equiv \left\langle {13 \atop 13} \right| H^{eff}_{3,\mathrm{CI}} \left| {13 \atop 13} \right\rangle$

(iv) For the off-diagonal matrix elements involving doubly excited configurations we set:

$\left\langle {i, i+1 \atop i, i+1} \right| H^{eff}_{N,\mathrm{CI}} \left| {i+1, i+2 \atop i+1, i+2} \right\rangle \equiv \left\langle {12 \atop 12} \right| H^{eff}_{3,\mathrm{CI}} \left| {23 \atop 23} \right\rangle$, for $|i-j|=1$ and $|k-l|=1$ $\left\langle {i, j \atop i, j} \right| H^{eff}_{N,\mathrm{CI}} \left| {k, l \atop k, l} \right\rangle \equiv 0$

for $|i-j|=1$ and $|i-l|=2$ $\left\langle {i, j \atop i, j} \right| H^{eff}_{N,\mathrm{CI}} \left| {i, l \atop i, l} \right\rangle \equiv \left\langle {12 \atop 12} \right| H^{eff}_{3,\mathrm{CI}} \left| {13 \atop 13} \right\rangle$. Hence MEb configurations only couple with MEu configurations of the same type of $|{13 \atop 13}\rangle$.

For $|i-j|>1$ and $|j-l|=1$, $\left\langle {i, j \atop i, j} \right| H^{eff}_{N,\mathrm{CI}} \left| {i, l \atop i, l} \right\rangle \equiv \left\langle {12 \atop 12} \right| H^{eff}_{3,\mathrm{CI}} \left| {13 \atop 13} \right\rangle$. I.e. $\left\langle {13 \atop 13} \right| H^{eff}_{N,\mathrm{CI}} \left| {14 \atop 14} \right\rangle \equiv \left\langle {12 \atop 12} \right| H^{eff}_{3,\mathrm{CI}} \left| {13 \atop 13} \right\rangle$, $\left\langle {14 \atop 14} \right| H^{eff}_{N,\mathrm{CI}} \left| {15 \atop 15} \right\rangle \equiv \left\langle {12 \atop 12} \right| H^{eff}_{3,\mathrm{CI}} \left| {13 \atop 13} \right\rangle$ and so on.

(v) For matrix elements involving singly and doubly excited configurations we set:

$\left\langle {1 \atop 1} \right| H^{eff}_{N,\mathrm{CI}} \left| {12 \atop 12} \right\rangle \equiv \left\langle {1 \atop 1} \right| H^{eff}_{3,\mathrm{CI}} \left| {12 \atop 12} \right\rangle$, $\left\langle {N \atop N} \right| H^{eff}_{N,\mathrm{CI}} \left| {N-1, N \atop N-1, N} \right\rangle \equiv \left\langle {3 \atop 3} \right| H^{eff}_{3,\mathrm{CI}} \left| {23 \atop 23} \right\rangle$. For $i \neq 1$ and $i \neq N$, $\left\langle {i \atop i} \right| H^{eff}_{N,\mathrm{CI}} \left| {i, i+1 \atop i, i+1} \right\rangle \equiv \left\langle {i \atop i} \right| H^{eff}_{N,\mathrm{CI}} \left| {i-1, i \atop i-1, i} \right\rangle \equiv \left(\left\langle {1 \atop 1} \right| H^{eff}_{3,\mathrm{CI}} \left| {12 \atop 12} \right\rangle + \left\langle {2 \atop 2} \right| H^{eff}_{\mathrm{CI}} \left| {23 \atop 23} \right\rangle \right)/2$.

Finally, $\left\langle {i \atop i} \right| H^{eff}_{N,\mathrm{CI}} \left| {i, i+2 \atop i, i+2} \right\rangle \equiv \left\langle {i \atop i} \right| H^{eff}_{N,\mathrm{CI}} \left| {i-2, i \atop i-2, i} \right\rangle = \left\langle {1 \atop 1} \right| H^{eff}_{3,\mathrm{CI}} \left| {13 \atop 13} \right\rangle$.

To summarize this section, we have first built an effective Hamiltonian for the trimer containing only the six configurations of interest that give the dominant contribution to the three Frenkel and three multiexcitonic states of the trimer. We have then used the matrix elements for the trimer to define the rules for building Hamiltonians for larger linear aggregates, which will be studied next. The approach is analogous to many tight binding schemes[59] or linear-scaling divide and conquer schemes[60] used for large scale electronic structure calculations with the main difference being that, in this case, we consider multi-electron rather than single electron wave-functions.

The accuracy of the partitioning method has been evaluated comparing the eigenvalues of the states of interest (S and ME states) for a linear tetramer obtained from a full SDCI Hamiltonian with the ones obtained with the matrix partitioning approach (the full set of data is reported in the **SI**). The root mean squared difference of the eigenvalues for the two different calculations is 0.007 eV, i.e. much smaller that the energy range (~0.7 eV) spanned by the states of interest.

2.5. Electronic structure of the 1D aggregate

Here we apply the method discussed in Section 2.4 to a decamer linear chain, whose eigenstates contain 10 S, 9 MEb and 36 MEu states, following the nomenclature introduced for the trimer case. In **Figure 3** we show the eingenvalue spectra results obtained for T (panel a) and P (panel b) scenarios at different values of F' and V_{ex}^{0}. The configuration content of each eigenstate was used to label them as S, MEb or MEu states (the mixing between these subgroups is minimal).

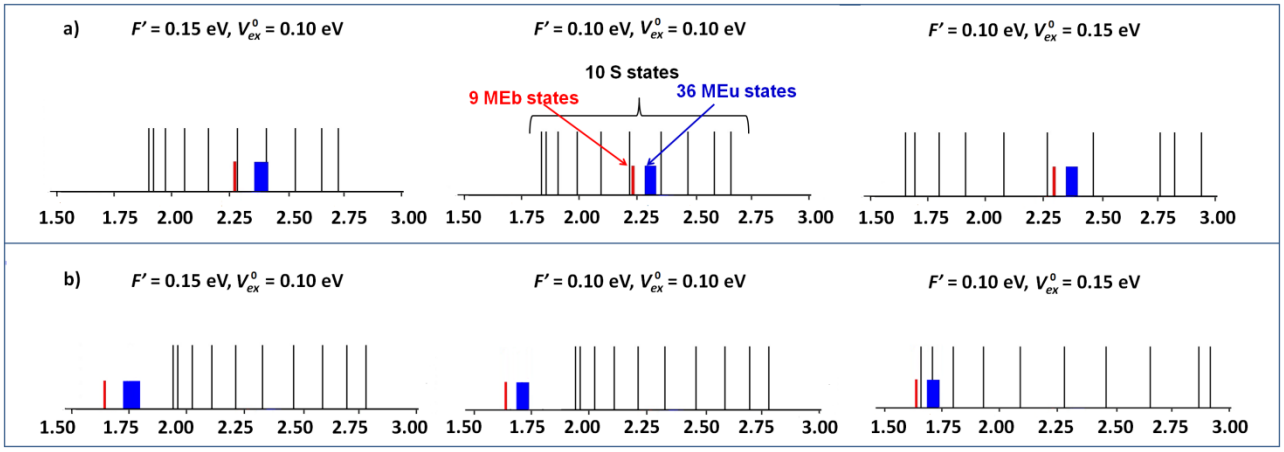

Figure 3: Spectrum of the eigenvalues for a decamer with indication of the different type of eigenstates S (long black lines), MEb (short red lines) and Meu (short blue lines) for a) a T choice of parameters b) a P choice of parameters, respectively.

First of all, we notice that, with ten monomers, we visualize two different bands. A singlet band, whose width is ruled by V_{ex}^{0} and two ME "bands" (for MEb and a MEu states respectively), whose width are much smaller and determined by the parameter F'. We use loosely the term "band" to describe the manifold of ME states for which band theory, based on a single electron picture, cannot be rigorously applied.

The main results of **Figure 3**, which is broadly valid for any plausible set of parameters, is that the Frenkel exciton band has a width of the order of hundreds of meV, an order of magnitude larger than the bandwidth of the MEu states (in the tens of meV). The MEb band is even narrower with bandwidth of just few meV. The narrowness of MEb and MEu "bands" has the dramatic consequence that these states are strongly localized by electron-phonon coupling. The reorganization energy for electronic transition between molecules of this size is invariably of the order of hundreds of meV, suggesting that the states within the MEb or MEu band are all localized on two molecules. If we consider the process of a ME state localized on sites (i, $i+1$) hopping into a neighboring ME state localized on sites ($i+1$, $i+2$), the reorganization energy of this process can be approximated as the twice the reorganization energy for a transition $T_1 \leftarrow S_0$ (because site i

undergoes to a geometry modification similar to a transition $S_0 \leftarrow T_1$ and site $i+2$ to a geometry modification similar to a transition $T_1 \leftarrow S_0$). The values estimated of reorganization energy for a transition $T_1 \leftarrow S_0$ in **SI** for pentacene and tetracene are 0.217 eV and 0.257 eV, respectively (see SI).

There are essentially two main results from the study of the electronic structure of aggregates leading to SF. First of all, there is not a unique SF but there are two possible pathways for SF, since there are two separated sets of ME states, that, for reasonable values of F', are also well separated in energy. The two processes will take place with different rates and it is reasonable to study them separately. Moreover, as the MEb are lower in energy, it is also conceivable that the energy difference between MEb and MEu plays the role of an activation energy for the separation of the triplets if they happen to be formed in the MEb state. Secondly both types of ME states are localized, therefore we can imagine SF as a process where there is a transition from a delocalized singlet state to a localized ME state. It would have been impossible to consider these features without a model capable of going beyond the description of a simple dimer, where there is only one ME state having no other option than being localized. The final step is to consider the dynamics of SF in molecular aggregates taking into account what has been learned on their electronic structure.

3. Dynamics of the ME$\leftarrow S_1$transition as a non-radiative decay

We aim at describing the dynamics of the transition from a delocalized S state to localized ME states in a linear chain of N monomers, adapting the formalism traditionally used for the study of non radiative decay and based on using Fermi golden rule (FGR).[61-64] This theoretical framework is among the simplest proposed to study SF but it allows a rapid quantitative assessment of the effect of the electronic structure described in the previous section on the dynamics of SF. Within this framework it is essential to consider explicitly the coupling between electronic states and a number (or all) nuclear degrees of freedom of the molecules. We perform this study in the limit of low temperature and we therefore consider only parameter sets where the SF is energetically favorable. We pinpoint that, while the comparison between different mechanisms proposed for SF in acenes is beyond the scope of this work, our model implicitly assumes that CT states are not intermediate states with a finite lifetime, but they just mediate the coupling between S and ME states. Hence, we explore the dynamics of SF within this mechanism. The steps followed in this section can be summarized as follows:(i) an evaluation of the electronic coupling between delocalized S states and localized ME states; (ii) a model for the Huang Rhys factors associated to the ME$\leftarrow S_1$ transition; (iii) an assessment of the validity of the FGR with different choices of the system parameters.

3.1. Calculation of the S_1-ME coupling

To study the dynamics of the transition from an initially prepared Frenkel exciton to a localized ME state, using time dependent perturbation theory, it is necessary to define an initial state that is not an eigenstate of the full Hamiltonian H_{CI}^{eff}. We are assuming that optical excitation only generates linear combinations of Frenkel states as the ME states are completely dark. We express the electronic Hamiltonian as the Hamiltonian of two separated families of states (S and ME) and their interaction. H_{CI}^{eff} can be written as:

$$H_{N,\mathrm{CI}}^{eff} = \ [H_{N,\mathrm{CI}}^{eff}]_{\mathrm{S}} + \ [H_{N,\mathrm{CI}}^{eff}]_{\mathrm{ME}} + V_{\mathrm{S-ME}} \tag{11}$$

Where the block matrices on the right hand site are defined as follow: (i) $[H_{N,\mathrm{CI}}^{eff}]_{\mathrm{S}}$ contains the matrix elements of the singlet configurations and the effective coupling among them, (ii) $[H_{N,\mathrm{CI}}^{eff}]_{\mathrm{ME}}$ contains the matrix elements of the ME configurations and the effective coupling among them; (iii) $V_{\mathrm{S-ME}}$ contains the coupling matrix elements between S and ME. Hence, if we want to describe $V_{\mathrm{S-ME}}$ as a perturbation, we define $[H_{N,\mathrm{CI}}^{eff}]_{\mathrm{S}}$ as the unperturbed Hamiltonian and *C* the matrix of the corresponding eigenvectors, which is a block diagonal matrix with the eigenvectors in one of the diagonal blocks and zeros elsewhere. The electronic couplings between delocalized S states and localized ME states is given by:

$$\bar{V}_{\mathrm{S-ME}} = C^{\dagger} V_{\mathrm{S-ME}} C \tag{12}$$

If we apply this method to $H_{3,\mathrm{CI}}^{eff}$ for the P scenario, we find that $\bar{V}_{\mathrm{S_1-ME_{12}}} = 0.019$ eV and $\bar{V}_{\mathrm{S_1-ME_{13}}} = 0.007$ eV, i.e. the coupling of S1 with MEb states (ME_{12}, ME_{23}) is larger than the coupling between S_1 and MEu. This is expected since MEb states couple, through CT configurations, with Frenkel-type configurations. On the other hand, MEu configurations couple more indirectly with Frenkel-type configurations via their coupling with doubly excited CT configurations at high energy, in turn coupled with MEb and S configurations. For large systems the coupling between S_1 and more separated multiexciton states is very small and so it is expected that S_1 will decay in either a MEb state or a MEu states where the pseudoptriplets are separated by one molecule.

Values of $\bar{V}_{\mathrm{s_1-ME}}$ depend on the size of the cluster also for ME states. This is reasonable since, as the Frenkel-type exciton is delocalized over N molecules, its coupling with localized ME states is

expected to decrease approximately as $1/\sqrt{N}$. In **Figure 4** we report values of $\bar{V}_{\mathrm{S_1-ME_{12}}}$ and $\bar{V}_{\mathrm{S_1-ME_{13}}}$ as a function of N, to show this dependence.

Figure 4:

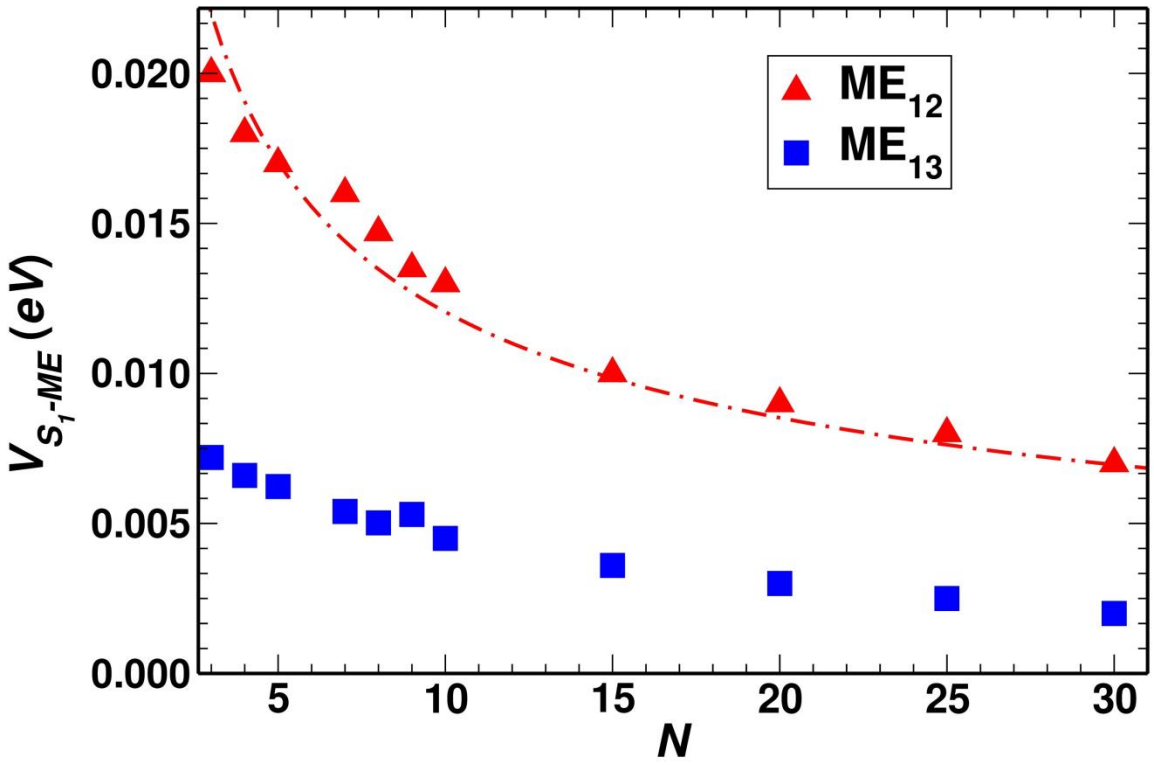

$\bar{V}_{s_1-\mathrm{ME}_{12}}$ and $\bar{V}_{s_1-\mathrm{ME}_{13}}$ as function of N ($F' = 0.15$ eV, $V_{ex}^0 = 0.10$ eV). Dotted line shows an appropriately scaled $1/\sqrt{N}$ function.

3.2. Vibronic Hamiltonian for singlet fission

We consider a molecular system with M electronic states and n vibrational degrees of freedom. The frequencies of these degrees of freedom are collected in the vector $\boldsymbol{\omega} = \{\omega_i\}$. The vibrational quantum numbers for each electronic state are collected in the vector $\mathbf{v} = \{v_i\}$. If we consider the case of the non radiative transition from an initially prepared S_1 state to $[N \times (N-1)]/2$ manifolds of vibronic ME states, in a cluster of N sites, each ME state is represented by $|\mathrm{ME}_{p,q}, \mathbf{v}\rangle$, where p and q are the electronic state indexes, denoting the sites where the two pseudo-triplets are located. We consider a simplified system where an initial S_1 state with no vibrational energy (denoted as $|\mathrm{S}_1, \mathbf{0}\rangle$ and of energy E_{S_1}) is coupled to a manifold of vibronic states $|\mathrm{ME}_{p,q}, \mathbf{v}\rangle$ of energy $E_{\mathrm{ME}_{pq}} + \hbar\mathbf{v}^{\mathrm{T}}\boldsymbol{\omega}$. The assumption implies that the zero point energy is included in the electronic energy and that the vibrational degrees of freedom are harmonic.

$$H_{el-vib} = H^0_{el-vib} + V_{el} \tag{13}$$

$$H^0_{el-vib} = E_{S_1}|S_1, \mathbf{0}\rangle\langle S_1, \mathbf{0}| + \sum_{p\neq q,\mathbf{v}} \left(E_{ME_{pq}} + \hbar \mathbf{v}^T \boldsymbol{\omega}\right) |ME_{pq}, \mathbf{v}\rangle\langle ME_{pq}, \mathbf{v}| \tag{14}$$

$$V_{el} = \sum_{p\neq q,\mathbf{v}} V_{p,q,\mathbf{v}} |ME_{p,q}, \mathbf{v}\rangle\langle S_1, \mathbf{0}| + h.c. \tag{15}$$

Assuming the validity of the Condon approximation, the coupling is the product of the electronic coupling and the Franck-Condon (FC) factor for the harmonic vibrations, that is known analytically. The squared modulus of the coupling is given by:

$$|V_{pq,\mathbf{v}}|^2 = |\bar{V}_{S_1-ME_{pq}}|^2 \cdot \prod_i \exp\left(-\sum_i \gamma_{i,ME_{pq}}\right) \frac{\gamma_{i,ME_{pq}}}{\nu_i!} \tag{16}$$

In the equation above $\gamma_{i,ME_{pq}}$ represents the Huang-Rhys factor for the i-th mode of the electronic transition 0→ME_{pq}, while $\bar{V}_{S_1-ME_{pq}}$ is the electronic coupling between initial state (S_1) and a final state ME_{pq}. If we assume that a generic cluster of N monomers behaves as in an Einstein's model for solids[65], where each monomer vibrates independently from each other, the excess energy of an electronic transition ME←S_1 can be distributed among the individual normal modes of each monomer; therefore the size of **ω** and **v** vectors is $N \times n$. The Huang Rhys factors are difficult to evaluate accurately for the ME←S_1 transition but they can be estimated sufficiently well if we consider that (i) the geometry of S_1 is almost identical to the one of S_0, because of delocalization of the S_1 state over several molecules, and (ii) that the ME state geometry can be taken to be close to the equilibrium geometry of two triplet states, because of localization of this type of state, as stated in Section 2.5. Therefore, the total number of active modes (along with the relative Huang-Rhys factors) for the ME← S_1 transition is given by twice the active normal modes of the T_1← S_0 transition in a single molecule (a set of normal modes on each pseudotriplets), each mode possessing the Huang-Rhys factor relative to the T_1← S_0 transition. Therefore, the number of modes n does not depend upon the size of the system, N, but it is always $2n$, making the calculations more feasible.

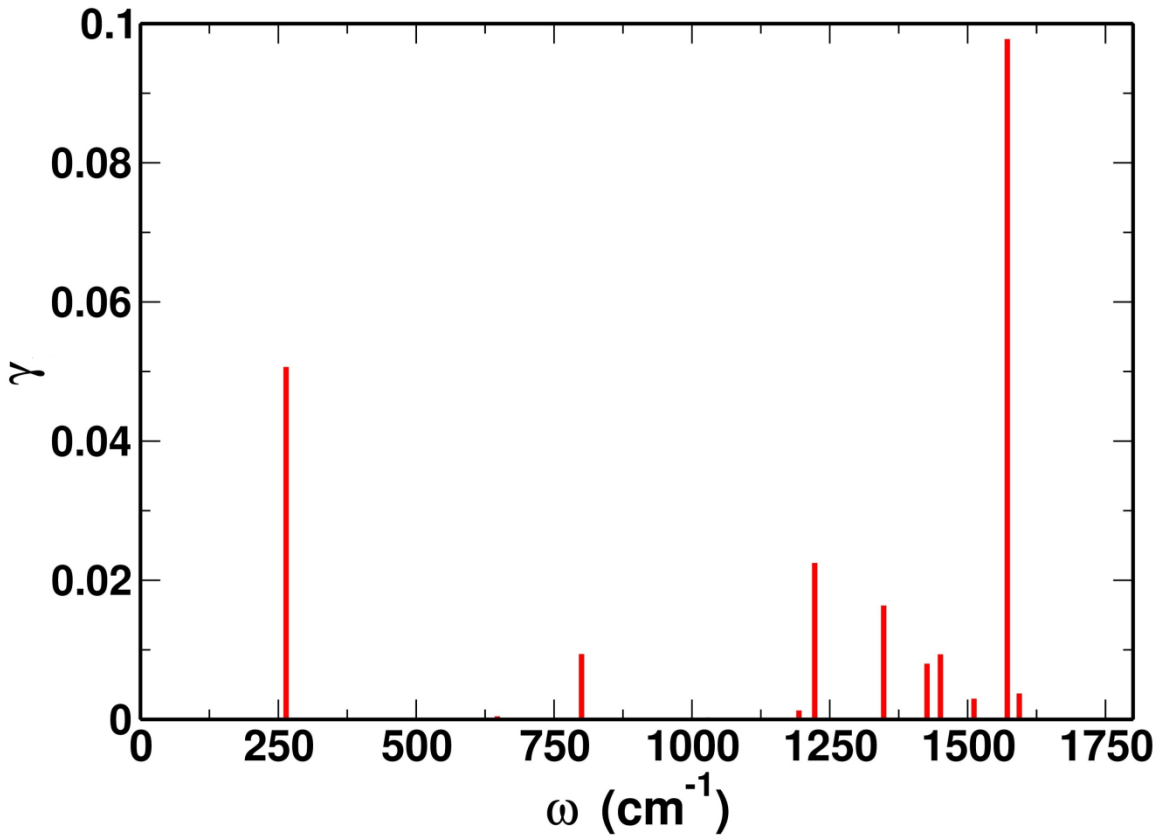

Figure 5: Huang Rhys factors (γ) for a single pentacene molecule for the normal mode of the corresponding frequency ω, for a $T_1 \leftarrow S_0$ electronic transition.

Huang Rhys factors for the $T_1 \leftarrow S_0$ transition have been computed at the B3LYP/6-31G* level of theory for an isolated pentacene molecule and these are reported, along with the corresponding frequency of the normal mode, in **Figure 5**. These values will be used in Section 3.3 to compute the Fermi golden rule rates.

3.3. Fermi golden rule for the study of the ME←S_1 transition

We study the dynamics of the transition from a delocalized S_1 state to $[N \times (N-1)]/2$ manifolds of localized ME states, using the FGR:

$$k_{\mathrm{tot}} = k_{\mathrm{S}_1,\mathbf{0}\rightarrow\{pq,\mathbf{v}\}} = \frac{2\pi}{\hbar} \sum_{p\neq q,\mathbf{v}} |V_{pq,\mathbf{v}}|^2 \delta\left[E_0 - \left(E_{\mathrm{ME}_{pq}} + \hbar \mathbf{v}^T \boldsymbol{\omega}\right)\right] \qquad (17)$$

k_{tot} can be also expressed as the sum of the contributions belonging to MEb and MEu states, respectively.

$$k_{\mathrm{tot}} = k_{\mathrm{MEb}} + k_{\mathrm{MEu}} \tag{18}$$

$\delta(x)$ is a delta Dirac function, which is approximated in its limit as a Gaussian function:

$$\frac{1}{\sqrt{2\pi}\sigma} e^{\frac{-(x)^2}{2\sigma^2}} \tag{19}$$

σ is a parameter ruling the width of the Gaussian, thus introducing a broadening to the energy of the final states. The vibrationally excited states in crystalline organic materials are broadened by depopulation and dephasing processes[66-68] and the typical vibrational broadening for polyacenes is of the order of ~0.25-0.40meV.[69-72] The FGR is not valid when the vibrational energy level spacing is larger than the broadening of the final levels, a condition that needs to be verified for the problem under study.

The singlet fission rate depends on the electronic coupling (evaluated in section 3.1), the Huang-Rhys factor (evaluated in section 3.2) and the energy difference between initial and final state. Given the semi-phenomenological nature of the model, rather than computing a single rate for singlet fission for the parameter set defined in the previous section we compute the rate as a function of the energy difference $\Delta E = E_{\mathrm{s}_1} - E_{\mathrm{MEb}}$ and we set the energy of the MEu states to be $E_{\mathrm{MEu}} = E_{\mathrm{MEb}} + 0.1$ eV. Leaving ΔE as a parameter is useful since the FGR for non-radiative transition can be used only for sufficiently large values ΔE.[73]

For the FGR approach to be valid, the rate should not depend on the magnitude of the broadening. If we plot the rate as a function of the broadening, it will reach a plateau at low values of σ. For even lower values of σ, $\log(k_{\mathrm{tot}})$ will diverge to $-\infty$. In **Figure 6** we show this behaviour, reporting k_{tot} against σ, at a fixed value of N (5) and different values of ΔE. For small energy gap ($\Delta E = 0.2$ eV) the FGR is valid for σ larger than approximately 0.40 meV, a value rather close to the broadening of vibrationally excited states in acenes (0.25-0.40 meV).[69-72] For larger ΔE, the value of σ becomes irrelevant within a large window of values. The results suggest that FGR is a suitable model for thermodynamically favorable singlet fission processes with ΔE~> 0.2 eV. To provide the rate in a standardized fashion for systems with different N and ΔE, the rate are given for the minimum value of σ (σ_{min}), which satisfy this inequality

$$\left| \frac{d^2 \mathrm{Log}(k_{\mathrm{tot}}/s^{-1})}{d(\mathrm{Log}\,\sigma\,/\mathrm{eV})^2} \right| < 10^{-4} \tag{20}$$

i.e. the smallest σ where the curvature of the function is sufficiently small.

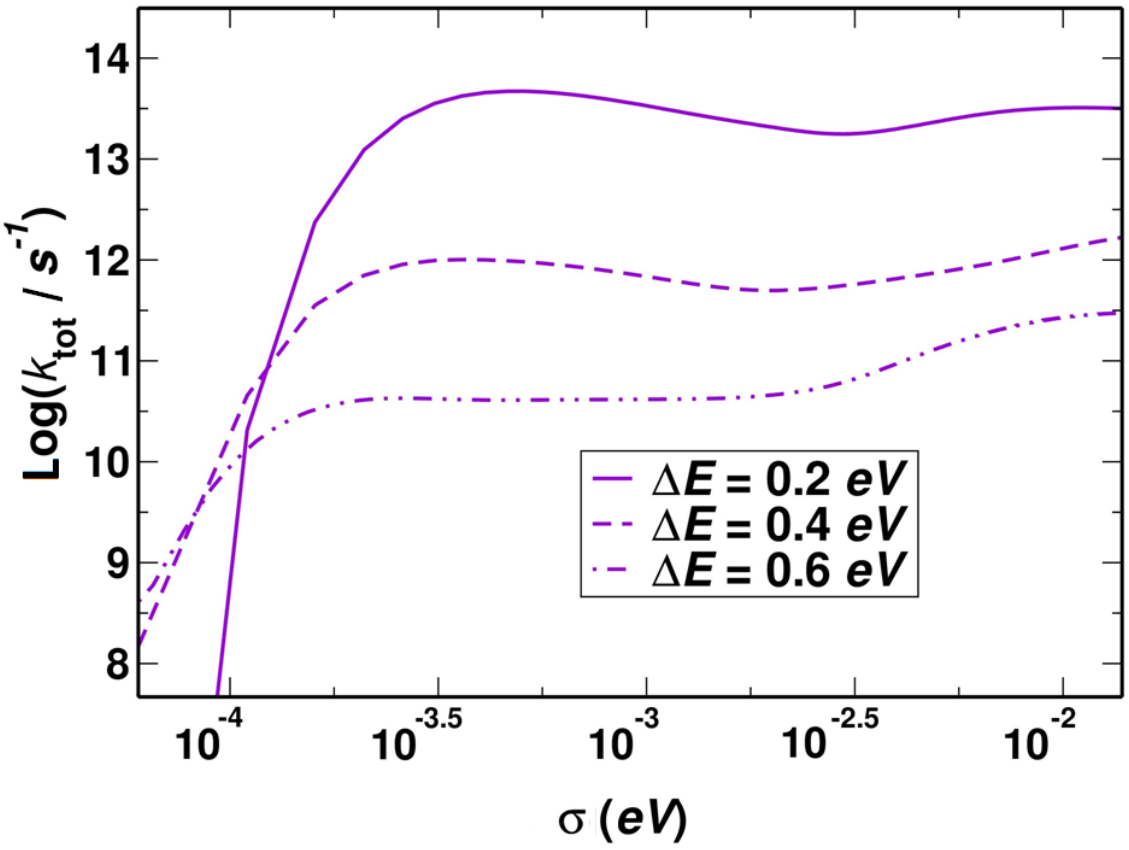

Figure 6: Log(k_{tot}) vs. σ at $N = 5$ for different values of ΔE.

In **Table 2** we collect values of σ_{min} and the relative k_{tot} for N =5, for different values of ΔE. The rates (and σ_{min}) decrease for larger values of ΔE, as predicted by energy gap law, because the density of states weighted by the Franck-Condon integrals decrease with increasing ΔE.

Table 2: $\sigma_{\min}$ and k_{tot} for different values of ΔE ($N = 5$)

ΔE (eV)	$-\text{Log}(\sigma_{\min}/\text{eV})$	$\text{Log}(k_{\text{tot}}/\text{s}^{-1})$
0.2	3.4	13.7
0.4	3.5	12.0
0.6	3.7	10.6

In **Figure 7** we report k_{MEb} and k_{MEu}, computed at $\sigma_{\min}$, as a function of N. Both k_{MEb} and k_{MEu} reach a constant value for N~>8 as the weakening of the electronic coupling is compensated by higher degeneracy, given by a larger number of MEb ($N-1$) and MEu states ($N-2$ for ME_{13}-type). Computed transition rates produce decay times between tens to hundreds of fs for 0.2 eV $<$ ΔE $<$ 0.4 eV.

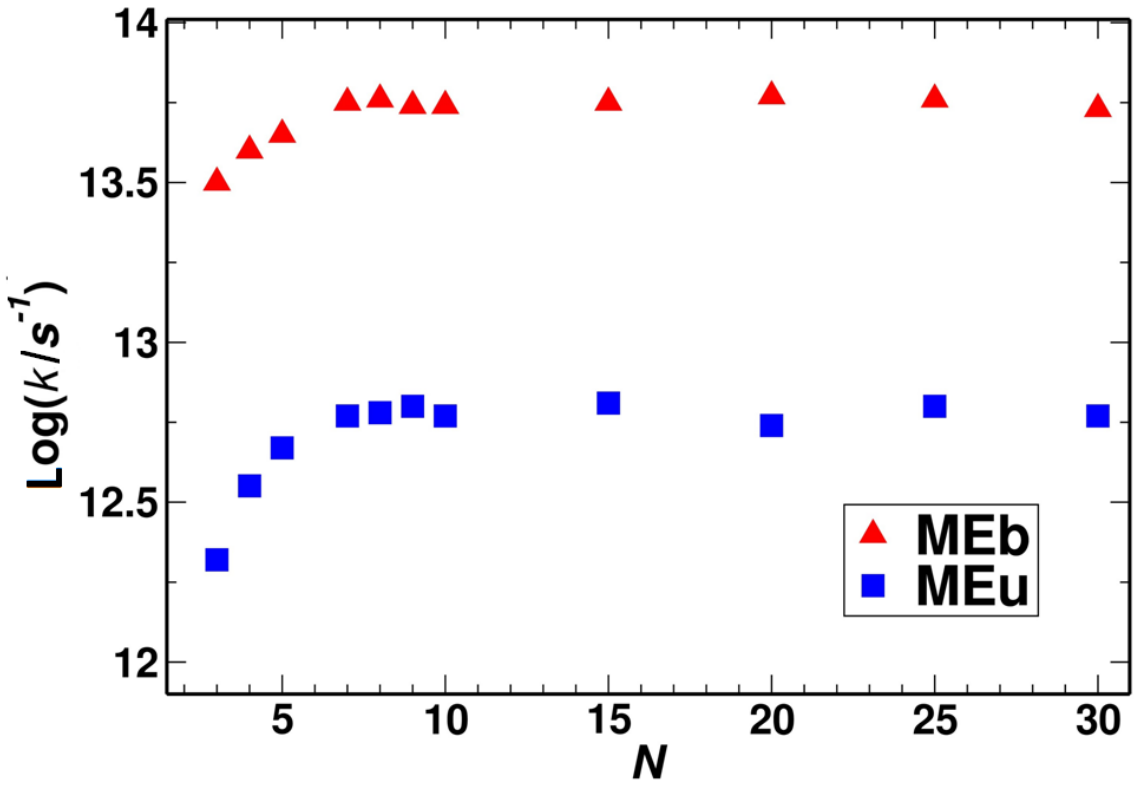

Figure 7: $\text{Log}(k_{\text{MEb}})$ and $\text{Log}(k_{\text{MEu}})$ as function of N ($\Delta E = 0.2$ eV).

It is interesting to study the branching of the rate between MEb and MEu states. We know that electronic coupling of MEb states with S_1 is stronger than the one relative to MEu states. On the other hand, MEu states should be favored for Franck Condon factors (energy is closer to S_1 and hence vibronic states with lower v are included). However, as the largest Huang-Rhys factors appear in the 1200-1600 cm^{-1} (~0.15-0.20 eV) interval (see **Figure 5**), this means that any ME manifold bringing states in resonance with S_1 will be favoured. The competition between the different effects leaves k_{MEb} one order of magnitude faster than k_{MEu} within this choice of system parameters.

This result is interesting because MEb states possess a binding energy, determined by the magnitude of the parameter F'. They are stabilized respect to the energy of two triplets ($E_{\mathrm{MEb}} < 2E_{\mathrm{T_1}}$), and their formation can slow down the final separation into two separate triplets. On the other hand, $E_{\mathrm{MEu}} \cong 2E_{\mathrm{T_1}}$, so singlets decaying over the MEu channel can produce two separate triplets without barrier. The parameter F' plays a crucial role in the SF also because $\bar{V}_{\mathrm{S_1-MEu}}$ and $\bar{V}_{\mathrm{S_1-MEb}}$ are determined by F', since the coupling between S and MEb states is mediated by CT states, through F' matrix elements.

Our calculations of electronic coupling $\bar{V}_{\mathrm{s_1-MEb}}$, derived by our phenomenological treatment, are somewhat in agreement (~ tens meV) with the ones computed in previous studies for the coupling between S_1 and ME in dimer models, based on *ab initio* calculations.[34, 42] Our computed rates for the ME←S_1 non radiative decay for a pentacene-like scenario at low ΔE are higher than the experimental[22] and theoretical[34, 42, 47] SF rates for pentacene crystals and dimer models, respectively. In particular, we obtain transition times of the order of tens fs, which are approximately one order of magnitude faster than SF times, obtained by Zhu and coworkers via time-resolved two-photon photoemission spectroscopy (>100 fs).[22] However, they also found that, as S_1 is depopulated, the rise in the population of the ME state is almost instantaneous, which is somewhat in agreement with our description of the ME←S_1 process, even if the interpretation of that experiment is debated and it could be an artifact.

While quantitative agreement is beyond the scope of this work, it is important to remark that the SF rate is very sensitive to changes of the F' parameters. As shown in detail in the **SI**, both k_{MEb} and k_{MEu} are proportional to the forth power of F'. If F' is reduced from 0.15 to 0.10 eV, the computed rate decreases by approximately one order of magnitude reconciling our results with other

theoretical works (100-500 fs).[34, 42, 47] A similar reduction of one order of magnitude in the rate is observed by keeping the absolute value of F' equal to 0.15 eV and changing sign of the Fock matrix elements in such a way that the coupling between HOMO orbitals has opposite sign than the coupling between LUMO orbitals (a result of negative interference between coupling paths). These observations collectively suggest that the accuracy of the Fock matrix elements is crucial if one is interested in quantitative evaluation of the rate for realistic system

Regardless of the specific choice of parameters, our model implies that the interpretation of the experimental results may be more complicated than previously thought. While other models assume that SF rate can be computed as the kinetic rate for the transition from the Frenkel exciton to the ME state in a dimer model, in our model, the *bound* ME, more rapidly produced at low ΔE, has to be converted in the *unbound* ME for the generation of almost free triplets. Hence, for a complete evaluation of the SF rate this second process should be also taken into account in the future. The overall approach is suitable for the study of 2D or 3D aggregates, but the number of parameters in that case is much larger and it is best to consider realistic systems with first principle evaluations of the relevant matrix elements rather than attempting a phenomenological description. We expect that the main observations of this work (i.e. localization of ME states and existence of different types of ME states) remain valid for aggregates of larger dimensionality. Both observations can be made only considering a model capable of going beyond the mere dimer picture.

4. Summary and Conclusions

In this paper we investigated the main difference introduced in the process of singlet fission when we consider an aggregate of molecules instead of a dimer. The main difficulty was to construct a reasonable model of the electronic structure of the molecular aggregate that describes reasonably well Frenkel, multi-excitonic and charge transfer states. For dimer and trimer system we have considered a model system fed with parameters that reproduce the main experimental or computational feature of well-studied systems such as pentacene or tetracene. For larger aggregates we have considered a reduced electronic configuration space and adopted a matrix partitioning method to construct the matrix elements of the Hamilton that take into account excluded configurations in an effective way.

The electronic structure calculations yield two main results:

(i) There are two energetically well separated multi-exciton states, that we have denoted as bound and unbound. The bound multi-exciton states have lower energy and are formed by configurations containing double excitations of neighboring molecule. It is possible to think to the energy difference between bound and unbound multi-exciton states as the barrier for separation of two triplets since the energy of the unbound multi-exciton state is essentially identical to that of two separated triplets.

(ii) The multi-exciton states are very weakly coupled, unlike the Frenkel states. Any reasonable value of the electron phonon coupling will localize these states forming a small exciton-polaron. In the aggregate, the transition between singlet and multi-exciton state is therefore a transition between a delocalized and a localized state.

To study the dynamics of singlet fission we resorted to the simplest possible theoretical framework. We considered the process as a non-radiative transition between the ground vibrational state of a Frenkel exciton and (several) manifolds of vibronic multi-exciton states. We performed our analysis using the Fermi Golden rule but the same Hamiltonian can form the basis for more advanced calculations if the parameter set is such that the Fermi Golden Rule cannot be applied.[46, 74, 75] The analysis of the results show that, as long as the energy difference between Frenkel and lowest-energy multi exciton state is larger than 0.2 eV the adopted theoretical model is valid. The computed rates are consistent with those observed experimentally. The model allows the computation of the branching ratio between the formation of bound and unbound multi-excitonic states indicating the former are generated with higher probability. The formation of two separate triplets is therefore likely to proceed initially via the formation of a bound multi-exciton state followed by formation (with a small energy barrier) of unbound multi-exciton that can become truly separated triplets when the spin coherence is loss.

In conclusion, the phenomenology of singlet fission is considerably richer when aggregates of molecules are considered. The proposed model represents an initial exploration of this phenomenology that must be complemented in the future with more system-specific electronic structure calculations and a quantum dynamics theory able to consider quasi-degenerate initial and final states.

Acknowledgements. We acknowledge financial support from the European Research Council (ERC). We are grateful to Dr. Juan Arago March for critically reading this manuscript and for useful discussions.

References

1. M. B. Smith and J. Michl, Chem. Rev. **110**, 6891 (2010).
2. M. B. Smith and J. Michl, Annu. Rev. Phys. Chem. **64**, 361 (2013).
3. M. W. B. Wilson, A. Rao, K. Johnson, S. Gélinas, R. di Pietro, J. Clark and R. H. Friend, J. Am. Chem. Soc. **135**, 16680 (2013).
4. P. J. Jadhav, A. Mohanty, J. Sussman, J. Lee and M. A. Baldo, Nano Lett. **11**, 1495 (2011).
5. J. J. Burdett and C. J. Bardeen, J. Am. Chem. Soc. **134**, 8597 (2012).
6. J. J. Burdett and C. J. Bardeen, Acc. Chem. Res **46**, 1312 (2013).
7. L. Ma, K. J. Tan, H. Jiang, C. Kloc, M.-E. Michel-Beyerle and G. G. Gurzadyan, J. Phys. Chem. A **118**, 838 (2014).
8. J. C. Johnson, A. J. Nozik and J. Michl, J. Am. Chem. Soc. **132**, 16302 (2010).
9. A. Rao, M. W. B. Wilson, S. Albert-Seifried, R. Di Pietro and R. H. Friend, Phys. Rev. B **84**,19541 (2011).
10. R. J. Dillon, G. B. Piland and C. J. Bardeen, J. Am. Chem. Soc. **135**, 17278 (2013).
11. A. J. Musser, M. Al-Hashimi, M. Maiuri, D. Brida, M. Heeney, G. Cerullo, R. H. Friend and J. Clark, J. Am. Chem. Soc. **135**, 12747 (2013).
12. B. Ehrler, M. W. B. Wilson, A. Rao, R. H. Friend and N. C. Greenham, Nano Lett. **12**, 1053 (2012).
13. B. J. Walker, A. J. Musser, D. Beljonne and R. H. Friend, Nat. Chem. **5**, 1019 (2013).
14. W. Shockley and H. J. Queisser, J. Appl. Phys. **32**, 510 (1961).
15. D. N. Congreve, J. Lee, N. J. Thompson, E. Hontz, S. R. Yost, P. D. Reusswig, M. E. Bahlke, S. Reineke, T. Van Voorhis and M. A. Baldo, Science **340**, 334 (2013).
16. K. Aryanpour, J. A. Muñoz and S. Mazumdar, J. Phys. Chem. C **117**, 4971 (2013).
17. P. M. Zimmerman, Z. Y. Zhang and C. B. Musgrave, Nat. Chem. **2**, 648 (2010).
18. P. M. Zimmerman, F. Bell, D. Casanova and M. Head-Gordon, J. Am. Chem. Soc. **133**, 19944 (2011).
19. A. Rao, M. W. B. Wilson, J. M. Hodgkiss, S. Albert-Seifried, H. Bassler and R. H. Friend, J. Am. Chem. Soc. **132**, 12698 (2010).
20. M. Tabachnyk, B. Ehrler, S. Bayliss, R. H. Friend and N. C. Greenham, Appl. Phys. Lett. **103**, 153302 (2013).
21. B. Ehrler, B. J. Walker, M. L. Bohm, M. W. B. Wilson, Y. Vaynzof, R. H. Friend and N. C. Greenham, Nat. Commun. **3**, 1019 (2012).
22. W.-L. Chan, M. Ligges, A. Jailaubekov, L. Kaake, L. Miaja-Avila and X.-Y. Zhu, Science **334**, 1541 (2011).
23. D. Beljonne, H. Yamagata, J. L. Brédas, F. C. Spano and Y. Olivier, Phys. Rev. Lett. **110**, 226402 (2013).
24. M. W. B. Wilson, A. Rao, J. Clark, R. S. S. Kumar, D. Brida, G. Cerullo and R. H. Friend, J. Am. Chem. Soc. **133**, 11830 (2011).
25. H. Marciniak, I. Pugliesi, B. Nickel and S. Lochbrunner, Phys. Rev. B **79**, 235318 (2009).
26. J. Lee, M. J. Bruzek, N. J. Thompson, M. Y. Sfeir, J. E. Anthony and M. A. Baldo, Adv. Mater. **25**, 1445 (2013).
27. R. Mondal, R. M. Adhikari, B. K. Shah and D. C. Neckers, Org. Lett. **9**, 2505 (2007).
28. M. M. Payne, S. R. Parkin and J. E. Anthony, J. Am. Chem. Soc. **127**, 8028 (2005).
29. B. Purushothaman, S. R. Parkin and J. E. Anthony, Org. Lett. **12**, 2060 (2010).
30. E. Busby, T. C. Berkelbach, B. Kumar, A. Chernikov, Y. Zhong, H. Hlaing, X.-Y. Zhu, T.F. Heinz, M. S. Hybertsen, M. Y. Sfeir, D. R. Reichman, C. Nuckolls and O. Yaffe, J. Chem. Am. Soc.**136**, 10654 (2014).

31. P. M. Zimmerman, C. B. Musgrave and M. Head-Gordon, Acc. Chem. Res. **46**, 1339 (2013).
32. W.-L. Chan, T. C. Berkelbach, M. R. Provorse, N. R. Monahan, J. R. Tritsch, M. S. Hybertsen, D. R. Reichman, J. Gao and X. Y. Zhu, Acc. Chem. Res. **46**, 1321 (2013).
33. T. C. Berkelbach, M. S. Hybertsen and D. R. Reichman, J. Chem. Phys. **138**, 114102 (2013).
34. T. C. Berkelbach, M. S. Hybertsen and D. R. Reichman, J. Chem. Phys. **138**, 114103 (2013).
35. F. Mirjani, N. Renaud, N. Gorczak and F. C. Grozema, J. Phys. Chem. C **118**, 14192 (2014).
36. D. Casanova, L. V. Slipchenko, A. I. Krylov and M. Head-Gordon, J. Chem. Phys. **130**, 044103 (2009).
37. D. Casanova, J. Chem. Theory Comput. **10**, 324 (2013).
38. Q. Wu, B. Kaduk and T. Van Voorhis, J. Chem. Phys. **130**, 034109 (2009).
39. J. Jortner and M. Bixon, J. Chem. Phys. **88**, 167 (1988).
40. M. Bixon and J. Jortner, J. Chem. Phys. **48**, 715 (1968).
41. M. Bixon and J. Jortner, J. Chem. Phys. **50**, 4061 (1969).
42. S. R. Yost, J. Lee, W. B. WilsonMark, T. Wu, D. P. McMahon, R. R. Parkhurst, N. J. Thompson, D. N. Congreve, A. Rao, K. Johnson, M. Y. Sfeir, M. Bawendi, T. M. Swager, R. H. Friend, M. A. Baldo and V. T. Voorhis, Nat. Chem. **6**, 492 (2014).
43. S. M. Parker, T. Seideman, M. A. Ratner and T. Shiozaki, J. Phys. Chem. C **118**, 12700 (2014).
44. A. V. Akimov and O. V. Prezhdo, J. Am. Chem. Soc. **136**, 1599 (2014).
45. W.-L. Chan, J. R. Tritsch and X. Y. Zhu, J. Am. Chem. Soc. **134**, 18295 (2012).
46. A. G. Redfield, IBM Journal of Research and Development **1**, 19 (1957).
47. T. C. Berkelbach, M. S. Hybertsen and D. R. Reichman, J. Chem. Phys. **141**, 074705 (2014).
48. X. Feng, A. V. Luzanov and A. I. Krylov, J. Phys. Chem. Lett. **4**, 3845 (2013).
49. H. Yamagata, J. Norton, E. Hontz, Y. Olivier, D. Beljonne, J. L. Brédas, R. J. Silbey and F. C. Spano, J. Chem. Phys. **134**, 204703 (2011).
50. L. Crocker, T. Wang and P. Kebarle, J. Am. Chem. Soc. **115**, 7818 (1993).
51. D. Stahl and F. Maquin, Chem. Phys. Lett. **108**, 613 (1984).
52. M. Kasha, H. Rawls and M. A. El-Bayoumi, Pure Appl. Chem **11**, 371 (1965).
53. A. Troisi and G. Orlandi, J. Phys. Chem. A **110**, 4065 (2006).
54. L. Sebastian, G. Weiser and H. Bassler, Chem. Phys. **61**, 125 (1981).
55. P. O. Löwdin, J. Chem. Phys. **19**, 1396 (1951).
56. P. O. Löwdin, J. Math. Phys. **3**, 969 (1962).
57. P.-O. Löwdin, J. Mol. Spectrosc. **10**, 12 (1963).
58. S. Priyadarshy, S. S. Skourtis, S. M. Risser and D. N. Beratan, J. Chem. Phys. **104**, 9473 (1996).
59. O. K. Andersen and O. Jepsen, Phys. Rev. Lett. **53**, 2571 (1984).
60. W. Yang, Phys. Rev. Lett. **66**, 1438 (1991).
61. J. Ulstrup and J. Jortner, J. Chem. Phys. **63**, 4358 (1975).
62. P. F. Barbara, T. J. Meyer and M. A. Ratner, J. Phys. Chem. **100**, 13148 (1996).
63. A. Nitzan, *Chemical Dynamics in Condensed Phases: Relaxation, Transfer and Reactions in Condensed Molecular Systems: Relaxation, Transfer and Reactions in Condensed Molecular Systems*. (Oxford University Press, **2006**).
64. K. V. Mikkelsen and M. A. Ratner, Chem. Rev. **87**, 113 (1987).
65. C. Kittel and P. McEuen, *Introduction to solid state physics*. (Wiley New York, 1986).
66. S. Dattagupta, *Relaxation phenomena in condensed matter physics*. (Elsevier, 2012).
67. S. Mukamel, Chem. Phys. **37**, 33 (1979).

68. S. Califano and V. Schettino, Int. Rev. Phys. Chem. **7**, 19 (1988).
69. J. C. Owrutsky, D. Raftery and R. M. Hochstrasser, Annu. Rev. Phys. Chem. **45**, 519 (1994).
70. C. Panero, R. Bini and V. Schettino, J. Chem. Phys. **100**, 7938 (1994).
71. R. W. Olson and M. D. Fayer, J. Phys. Chem. **84**, 2001 (1980).
72. C. L. Schosser and D. D. Dlott, J. Chem. Phys **80**, 1394 (1984).
73. R. Englman and J. Jortner, Mol. Phys. **18**, 145 (1970).
74. F. Petruccione and H.-P. Breuer, *The theory of open quantum systems*. (Oxford Univ. Press, 2002).
75. V. May and O. Kühn, *Charge and energy transfer dynamics in molecular systems.* (John Wiley & Sons, 2008).